

Modified Phase-Shift Analysis of the $I=0$ K - N System and the Existence of Exotic Baryon Resonances*

R. Aaron†

*Los Alamos Scientific Laboratory, University of California, Los Alamos, New Mexico 87544 and
Department of Physics, Northeastern University, Boston, Massachusetts 02115*

and

M. Rich

Los Alamos Scientific Laboratory, University of California, Los Alamos, New Mexico 87544

and

W. L. Hogan and Y. N. Srivastava

Department of Physics, Northeastern University, Boston, Massachusetts 02115

(Received 7 August 1972; revised manuscript received 25 October 1972)

We have performed a modified phase-shift analysis of the $Y=2$, $I=0$ K - N system and find convincing evidence for exotic resonances in the $D_{3/2}$ and either $S_{1/2}$ or $P_{1/2}$ states. Using finite-energy sum rules, we further show that, contrary to popular notions, our results are consistent with the degree of exchange-degeneracy breaking allowed by the present experimental data.

I. INTRODUCTION

We have performed an energy-dependent modified phase-shift analysis of the $I=0$ K - N system in the region $P_{\text{lab}} = 640$ – 1585 MeV/ c . Experimental input includes charge-exchange ($K^+ + n \rightarrow K^0 + p$) angular distributions,¹ $I=0$ total cross sections,¹ and the results of a charge-exchange polarization measurement at 600 MeV/ c .² In addition, we use $I=1$ phase shifts from previous studies of the $K^+ - p$ system.³ Our approach differs from others in two ways: (1) We include in the analysis F and G partial waves which we claim are required by theoretical considerations. (2) In all partial waves excepting $S_{1/2}$ and $P_{1/2}$ the inelasticity parameters (η 's) are obtained from the calculation of Aaron, Amado, and Silbar (AAS).⁴ We obtain $I=0$ phase-shift solutions which fit 374 data points with a $\chi^2 \approx 560$ for 353 degrees of freedom (DOF). All those solutions which are consistent with the low-energy polarization experiment at 600 MeV/ c and agree with previous $I=0$ phase-shift analyses at low energies contain $D_{3/2}$ and either $S_{1/2}$ or $P_{1/2}$ exotic resonances. We demonstrate that polarization measurements would be very helpful in demonstrating the existence of these resonances. Examination of finite-energy sum rules for the charge-exchange amplitude shows that our exotic resonances do not upset ρ - A_2 exchange degeneracy

to an extent greater than presently allowed by experimental evidence.

Our approach is motivated by the work of AAS, who argued that dynamical mechanisms which produce resonances in the π - N system are also present in the K - N system. In particular, ρ - N intermediate states drive the $D_{13}(1520)$ π - N resonance and also contribute importantly to the $S_{11}(1700)$ π - N state.⁵ Including $K^*(890)$ - N intermediate states in the context of relativistic three-body equations, AAS analogously obtain exotic $D_{3/2}$ and $S_{1/2}$ resonances in the $I=0$ K - N system where isospin factors are favorable. While certain results of the above calculation are only qualitative, others are quantitative and we shall use them in our phase-shift analysis below.

In Fig. 1 we show the "box" mechanism which serves as a potential for the integral equations of AAS. Because of isotopic-spin factors it is nine times larger in the $I=0$ state than in the $I=1$ state. It provides the longest-range inelastic force in the $I=0$ K - N system and, according to AAS, drives resonances in the $S_{1/2}$ and $D_{3/2}$ states. There is one free parameter in the calculation of AAS, and it is chosen to give correctly the single-pion production cross section. The dominance of the K^* box mechanism is consistent with the experimentally observed dominance of single-pion production by K^* - N states.

We feel that the box mechanism of Fig. 1 should play a role in a K - N phase-shift analysis analogous to the crucial role played by one-pion exchange (OPE) in an analysis of nucleon-nucleon scattering. There is an important difference between the above two mechanisms – OPE determines the high partial waves in NN scattering, but the K^* box determines only the imaginary parts of the high partial waves (and thus the η 's) in K - N scattering. Other diagrams, such as, for example, ρ exchange, contribute importantly to the real parts. We therefore assume that except in the $S_{1/2}$ and $P_{1/2}$ states (where short-range forces can be particularly important) the AAS model gives the correct inelasticity parameters (η 's), and we use these in the ensuing phase-shift analysis.⁶ It is true that in a definitive phase-shift analysis the inelasticities would be determined from the data and not from a theoretical model. On the other hand, the relatively small amount and poor quality of the data does not permit such an elaborate analysis while at the same time including the effects of F and G waves as required by the presence of the box mechanism. An important prediction of AAS is that high partial waves, particularly $F_{5/2}$ and $G_{7/2}$, contribute importantly to K^* production above $P_{\text{lab}} \approx 1.3$ GeV/ c and thus via unitarity to elastic K - N scattering. For example, at $P_{\text{lab}} = 1.37$ GeV/ c , F and G waves contribute $\sim 22\%$ of the total inelastic cross section. The presence of high partial waves in K^* production is consistent with the strongly forward-peaked K^* - N angular distributions observed by Hirata *et al.*⁷

II. $I=0$ PHASE-SHIFT ANALYSIS

Parametrizing the $I=1$ and $I=0$ K - N scattering amplitudes (A_1 and A_0 , respectively), we now attempt to fit 374 data points including 14 total $I=0$ cross-section measurements and 360 charge-exchange ($K^+ + n \rightarrow K^0 + p$) angular distribution data at 17 energies. The charge-exchange amplitude is $A_{\text{CEX}} = \frac{1}{2}(A_1 - A_0)$. The amplitudes A_1 and A_0 are expressed in terms of real phase shifts and inelasticity parameters. The $I=1$ δ 's and η 's are obtained from previous analyses of the $K^+ - p$ system.³ The following results are independent of which set of $I=1$ phase shifts are used. In the $I=0$

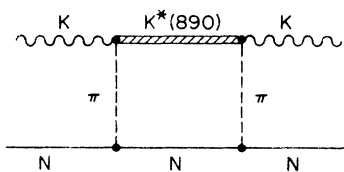


FIG. 1. Box mechanism.

system the η 's are obtained from the model of AAS as described above, while the phase shifts are parametrized in the form

$$\delta_{J,l} = k^{2l+1} [a_0(J,l) + a_2(J,l)k^2 + a_4(J,l)k^4]. \quad (1)$$

For partial waves other than $S_{1/2}$, $P_{1/2}$, and $D_{3/2}$, a_4 is set equal to zero; thus, we use a total of 21 parameters. The above parametrization may be somewhat restrictive but is sufficient for our purposes and justified by the resulting low χ^2/DOF .

Thus, with the η 's fixed by AAS and the δ 's free to vary, we perform a standard χ^2 analysis. There is little theoretical justification for accepting the η 's of AAS in the $S_{1/2}$ and $P_{1/2}$ states, since the phase shifts are large and particularly susceptible to short-range forces not included in their calculation. Therefore, in principle, we should free $\eta_{S_{1/2}}$ and $\eta_{P_{1/2}}$ and allow them to vary freely, constrained only by the total inelastic cross section. The relatively poor quality of the data does not warrant this procedure. However, in order to be more general and allow inelasticity in the $P_{1/2}$ wave, we arbitrarily exchange the $S_{1/2}$ and $P_{1/2}$ η 's of AAS (this procedure maintains the inelastic cross section) and again search for solutions. We find two classes of solutions, one with a resonant $D_{3/2}$ wave and the other with a nonresonant $D_{3/2}$ wave, that fit 374 data points with $\chi^2 \approx 560$ for 353 DOF. Typical solutions A, B (resonant $D_{3/2}$), and C (nonresonant $D_{3/2}$) are shown in Table I. Argand diagrams and speeds for the resonant partial waves in solutions A and B are displayed in Figs. 2 and 3. Both solutions have clear $D_{3/2}$ resonances at $W \approx 1830$ MeV with widths $\Gamma \approx 100$ MeV. Solutions A and B show weaker resonance activity in the $S_{1/2}$ and $P_{1/2}$ channels, respectively, the resonance interpretation being less evident from our speed plots. However, at very least, there is considerable structure in these partial waves (whether or not there are poles on the second sheet) unlike the flat predictions from the (simple) quark models and duality. These exotic ("resonance") activ-

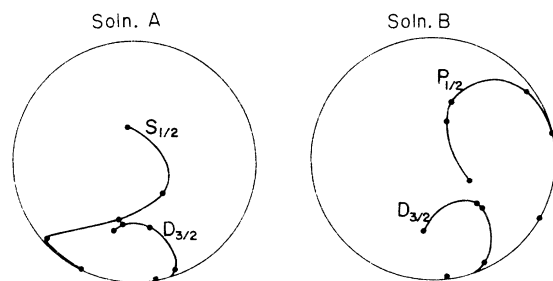


FIG. 2. Argand diagrams for resonant phase shifts in Soln. A and Soln. B of Table I. The five reference dots are at 1625, 1780, 1892, 1961, and 2059 MeV.

TABLE I. Two typical resonant solutions, Soln. A and Soln. B, and a nonresonant solution, Soln. C, are tabulated. Results of a few previous analyses are also shown. For each partial wave at a given lab momentum we give the phase shift δ (degrees) and the corresponding η below it.

	P_{lab} (MeV/c)	$S_{1/2}$	$P_{1/2}$	$P_{3/2}$	$D_{3/2}$	$D_{5/2}$	$F_{5/2}$	$F_{7/2}$	$G_{7/2}$	$G_{9/2}$
Soln. A, $\chi^2 = 559$	640	-13.6	39.1	-6.8	5.5	-2.3	0.9			
		1.0	1.0	1.0	1.0	1.0	1.0			
	865	-23.8	53.3	-9.7	9.4	-5.0	2.9	-1.0	0.4	-0.2
		0.998	1.0	1.0	0.998	1.0	1.0	1.0	1.0	1.0
	970	-25.0	57.3	-10.5	10.2	-6.5	4.5	-1.5	0.7	-0.3
		0.968	1.0	1.0	0.964	1.0	1.0	1.0	1.0	1.0
	1210	-8.5	56.7	-9.0	6.0	-7.9	7.5	-2.8	1.5	-0.8
		0.505	0.935	0.981	0.560	1.0	0.942	1.0	0.992	1.0
	1365	21.2	51.5	-4.8	-7.4	-5.3	5.8	-2.9	1.1	-1.1
		0.342	0.860	0.957	0.533	0.994	0.889	1.0	0.976	1.0
	1585	96.4	46.1	6.8	-8.2	7.2	-10.6	3.8	-4.5	-1.3
		0.303	0.769	0.931	0.604	0.986	0.851	1.0	0.955	1.0
Soln. B, $\chi^2 = 563$	640	2.5	29.2	-3.5	2.3	-3.1	0.6			
		1.0	1.0	1.0	1.0	1.0	1.0			
	865	-9.1	50.7	-5.1	7.6	-7.0	1.9	-0.2	0.4	-0.7
		1.0	0.998	1.0	0.998	1.0	1.0	1.0	1.0	1.0
	970	-13.0	62.0	-5.5	11.9	-9.2	2.9	-0.3	0.7	-1.4
		1.0	0.968	1.0	0.964	1.0	1.0	1.0	1.0	1.0
	1210	-8.1	79.8	-4.9	21.8	-12.6	4.5	0.3	1.6	-3.8
		0.935	0.505	0.981	0.560	1.0	0.942	1.0	0.992	1.0
	1365	9.4	78.7	-2.9	21.9	-11.1	2.9	1.8	1.3	-5.0
		0.860	0.342	0.957	0.533	0.994	0.889	1.0	0.976	1.0
	1585	60.2	47.5	2.9	-6.1	1.1	-9.4	7.4	-4.2	-1.7
		0.769	0.303	0.931	0.604	0.986	0.851	1.0	0.955	1.0
Soln. C, $\chi^2 = 603$	640	26.4	6.3	2.5	-1.7	-2.9	0.5	-0.8		
		1.0	1.0	1.0	1.0	1.0	1.0	1.0		
	865	52.3	16.9	3.5	-3.4	-6.3	1.6	-2.8	0.6	-0.5
		0.998	1.0	1.0	0.998	1.0	1.0	1.0	1.0	1.0
	970	59.1	24.3	3.7	-4.3	-8.2	2.5	-4.3	1.1	-0.9
		0.968	1.0	1.0	0.964	1.0	1.0	1.0	1.0	1.0
	1210	41.2	42.4	3.0	-5.3	-9.9	4.2	-7.4	2.4	-2.3
		0.505	0.935	0.981	0.560	1.0	0.942	1.0	0.992	1.0
	1365	-4.7	50.8	1.3	-4.9	-6.7	3.3	-6.5	1.7	-3.0
		0.342	0.860	0.957	0.533	0.994	0.889	1.0	0.976	1.0
	1585	-130.1	49.1	-3.4	-3.4	9.1	-5.4	7.0	-7.4	-7.9
		0.303	0.769	0.931	0.604	0.986	0.851	1.0	0.955	1.0
Hirata <i>et al.</i>	865	-12.7 ± 5.9	65.2 ± 2.5	5.3 ± 3.6	9.4 ± 2.2	-7.1 ± 3.4				
		0.980	0.984	0.992	0.989	0.994				
	970	-6.6 ± 3.9	72.2 ± 5.0	10.1 ± 4.4	13.8 ± 3.3	-10.7 ± 2.9				
		0.944	0.926	0.969	0.981	0.987				
Ray <i>et al.</i>	600	13.2 ± 6.6	31.8 ± 6.4	-2.6 ± 2.4	-2.3 ± 2.4	-0.9 ± 1.0				
Soln. 2		1.0	1.0	1.0	1.0	1.0				

ities are our principal and striking results which tend to cast severe doubt upon the validity of these other models.

In many ways our phase shifts are similar to the acceptable solutions in the comprehensive analysis of the BGRT collaboration.⁸ Only the resonant solutions are consistent with previous phase-shift analyses and the low-energy polarization measurements of Ray *et al.*² We have not used the latter polarization data in our χ^2 analysis. We feel that

it is probably more independent than much of the angular distribution data and should be given a much higher weighting. Because of the few data and large associated errors we have decided to use the polarization data in a qualitative way as a yes-or-no criterion – i.e., we accept solutions with large negative polarizations at low energies and discard solutions with essentially zero polarizations at these energies. In Fig. 4 we display predicted polarizations at 640, 970, 1365, and

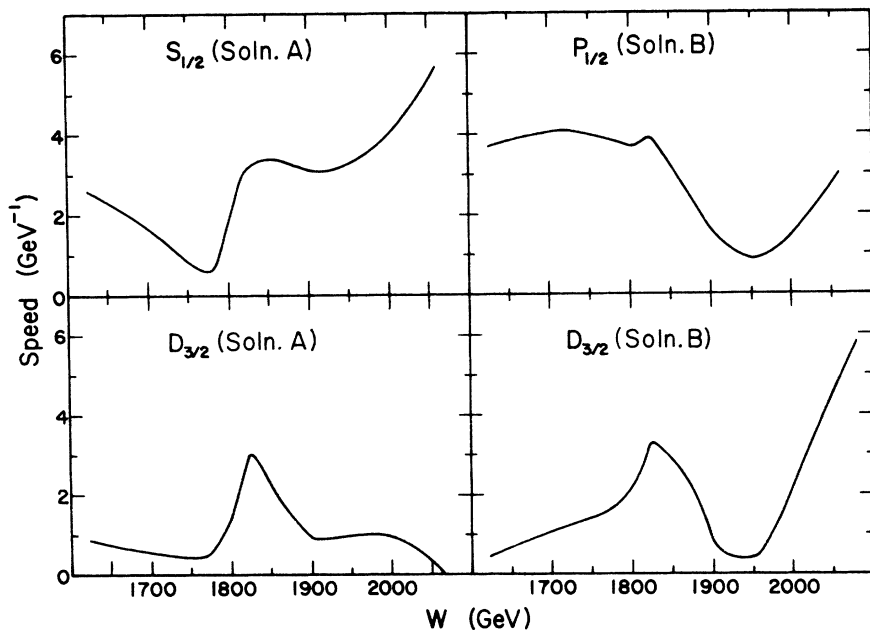


FIG. 3. Speeds corresponding to Argand diagrams of Fig. 2.

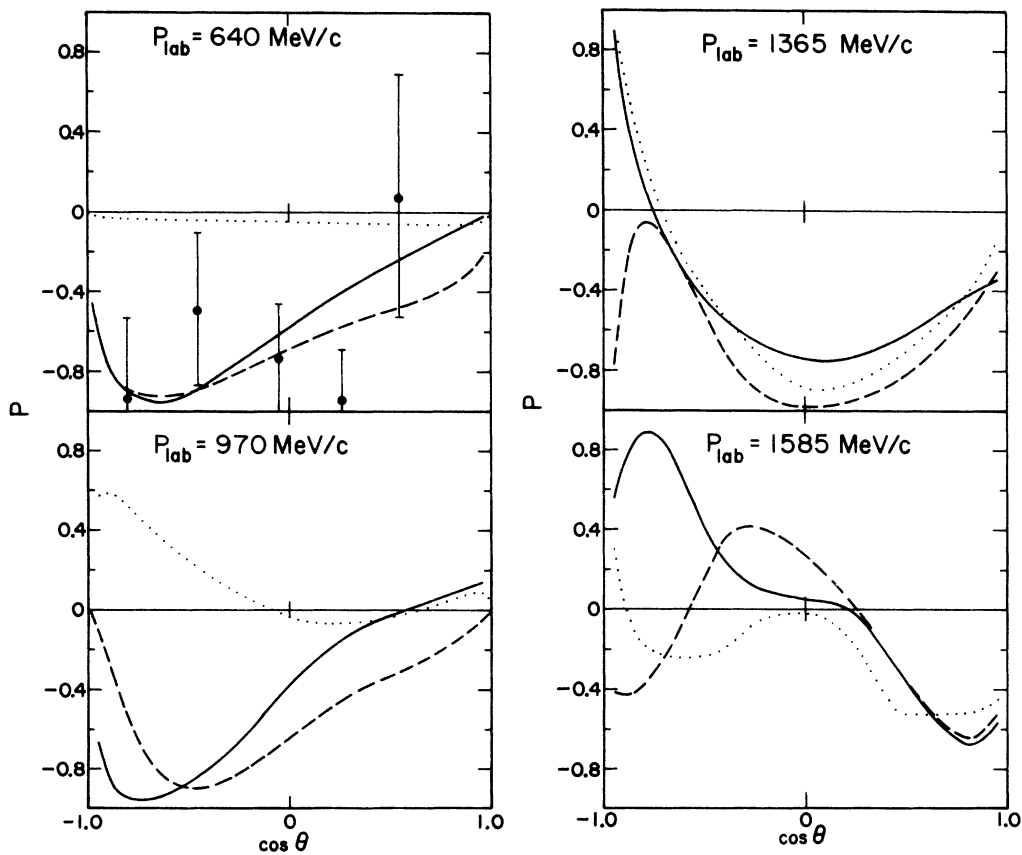


FIG. 4. Polarizations P corresponding to Soln. A (—), Soln. B (---), and Soln. C (···) of Table I at $P_{\text{lab}} = 640, 970, 1365,$ and 1585 MeV/c vs cosine of scattering angle θ . The data points are those of Ray *et al.* (Ref. 2) obtained at 600 MeV/c. Also, the sign convention for P is that of Ray *et al.*

1585 MeV/c. It is clear that the resonant and non-resonant solutions give dramatically different polarizations, and thus that polarization measurements in the energy region of our analyses would help distinguish between solutions.

We now examine finite-energy sum rules (FESR) for K - N charge-exchange (CEX) scattering – these provide theoretical arguments for ρ - A_2 exchange degeneracy. In standard notation we may write the FESR for the A' K - N CEX amplitudes in the form^{9,10}

$$\int_0^{\nu_0} d\nu \text{Im}(A'_1 - A'_0) = \int_0^{\nu_0} d\nu (-2\rho + 2A_2 + \Delta), \quad (2)$$

where $\nu = (s - u)/4m$ and Δ represents all secondary Regge contributions. Previous Regge-pole analyses¹¹ indicate that a degenerate ρ - A_2 pair alone is not sufficient to describe the high-energy data for the K - N and \bar{K} - N systems. The difference of the ρ and A_2 Regge terms in these nondegenerate fits should give a measure of Δ . For small Δ , the exotic $I=0$ K - N resonances that we predict might upset the equality in Eq. (2) by contributing to the left-hand side. However, this need not be the case, since there is cancellation between the $I=0$ and $I=1$ amplitudes and among the various partial waves. In fact, our phase-shift analysis gives results consistent with high-energy Regge fits. In Fig. 5, for $t = -0.05$ GeV² we compare $\text{Im}A'$ with R , the imaginary part of the high-energy Regge-pole fit of Dass, Michael, and Phillips¹² extrapolated to low energies. They use nondegenerate ρ and A_2 poles to fit the data – the separate ρ and A_2 contributions are much larger in magnitude than R itself. It is significant that our calculated low-energy amplitude (i) changes sign, and (ii) is comparable in magnitude to R and tends to average it in the sense of FESR duality. While the above results are not precise enough to provide criteria for the selection of preferred phase-shift solutions, they do provide qualitative evidence that our exotic resonances need not conflict with weak ρ - A_2 exchange degeneracy.

It is worth mentioning here that we also projected parity-conserving partial waves from four Regge fits¹³ to the K - N and \bar{K} - N system and plotted their Argand diagrams. Although most waves yielded no useful information, it is interesting that we obtained resonance-type loops in the D_{03} wave for each of the fits we tried.

III. CONCLUSIONS

We have performed a semiphenomenological phase-shift analysis using experimental and theo-

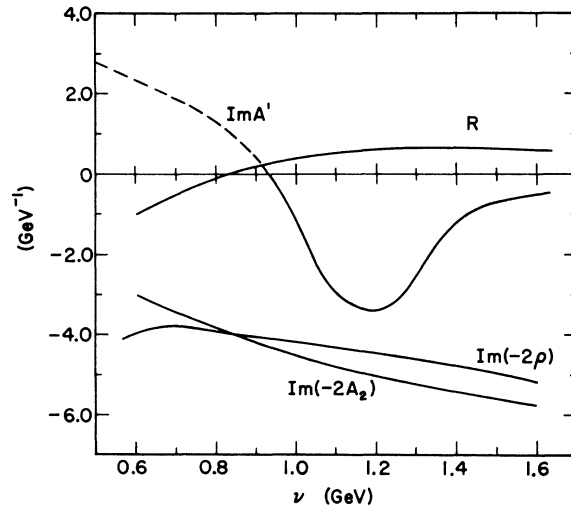


FIG. 5. Comparison of $\text{Im}A'$ (calculated with Soln. A) with $R = \text{Im}(-2\rho + 2A_2)$ for $t = -0.05$ GeV². $\text{Im}(-2\rho)$ and $\text{Im}(-2A_2)$ are plotted separately to show the large cancellation occurring. The dashed part of $\text{Im}A'$ is that below $P_{\text{lab}} = 640$ MeV/c and is obtained by extrapolating Eq. (1). All solutions give roughly the same curve. At threshold $\nu = m_K$.

retical input. It was necessary to use theory in order to keep the number of solutions manageable and at the same time include F and G partial waves as required by the long-range part of the K - N interaction (i.e., the K^* box of Fig. 1). We obtain fits to 374 data points with $\chi^2/\text{DOF} \approx 1.6$. Within the constraints of relatively limited and poor data, we claim the existence of $Y=2$, $I=0$ exotic resonances in the D_{03} and either S_{01} or P_{01} states. We further provide qualitative evidence that these resonances do not conflict with weak ρ - A_2 exchange degeneracy. We suggest polarization measurements to help clarify the situation.

The fact that we fit the data as well as we do using the η 's of AAS is in some sense a confirmation of the major features of their model. It is true that the more sophisticated BGRT⁸ analysis obtains better fits to the K - N charge-exchange data than we do ($\chi^2/\text{DOF} \approx 1.1$ – 1.2). On the other hand, they do not include partial waves higher than D in their analysis, and it is conceivable, for example, that their solutions at higher energies might be ruled out by careful polarization measurements.

Finally, the present K - N data, such as they are, do seem to imply at least one (and perhaps two) resonance(s), in conflict with popular notions like the (simple) quark model and exact exchange degeneracy. On the other hand, strong prejudices derived from these latter notions have discouraged

experimentalists from seeking new data. We hope to have convinced the reader how absolutely crucial it is to obtain new and accurate data in the

$I=0$ K - N system in order to decide on the validity of some of the more widely held beliefs in high-energy physics.

*Work supported in part by the Atomic Energy Commission and the National Science Foundation.

†Permanent address: Northeastern University, Boston, Massachusetts 02115.

¹A. A. Hirata *et al.*, LBL Report No. UCRL-20243, 1971 (unpublished); Bologna-Glasgow-Roma-Trieste Collaboration (BGRT), Nucl. Phys. **B42**, 437 (1972); L. R. Price *et al.*, LBL Report No. UCRL-20000 K^+N , 1969 (unpublished).

²A. K. Ray *et al.*, Phys. Rev. **183**, 1183 (1969).

³S. Kato *et al.*, ANL Report No. ANL/HEP 7115, 1971 (unpublished); G. A. Rebka *et al.*, Phys. Rev. Letters **24**, 160 (1970); R. E. Cutkosky and B. B. Deo, Phys. Rev. **D 1**, 2547 (1970).

⁴R. Aaron, R. D. Amado, and R. R. Silbar, Phys. Rev. Letters **26**, 407 (1971).

⁵R. Aaron and R. D. Amado, Phys. Rev. Letters **27**, 1316 (1971).

⁶The AAS η 's in the $S_{1/2}$, $P_{1/2}$, and $D_{3/2}$ states are obtained by solving integral equations. In all other partial waves the η 's may be obtained from the first-order diagrams, i.e., the imaginary part of the box.

⁷A. A. Hirata *et al.*, Phys. Rev. Letters **21**, 485 (1968);

and in *Hyperon Resonances - 70*, edited by E. C. Fowler (Moore, Durham, N. C., 1970), p. 429.

⁸BGRT Collaboration, Nucl. Phys. **B42**, 445 (1972).

⁹We consider only the A' amplitude since there is evidence that the nonsense-wrong-signature fixed-pole contributions to A' are small, particularly in the forward direction, while the B amplitude appears to require at least one fixed pole; cf. Ref. 9.

¹⁰M. Dubovoy, Phys. Rev. **D 5**, 193 (1972).

¹¹D. Cline and J. Matos, Nucl. Phys. **B37**, 161 (1972); G. V. Dass, C. Michael, and R. J. N. Phillips, *ibid.* **B9**, 549 (1969); R. J. N. Phillips and W. Rarita, Phys. Rev. **139**, B1336 (1965); W. Rarita and B. Schwarzschild, *ibid.* **162**, 1378 (1967). For an extensive listing of Regge models for the K - N and \bar{K} - N system, see Table 5 in the review by P. D. B. Collins, Phys. Reports **1C**, No. 4 (1971).

¹²Dass, Michael, and Phillips, Nucl. Phys. **B9**, 549 (1969). We choose their solution (b) of Table I, since that is the one that comes closest to exchange degeneracy.

¹³Dass, Michael, and Phillips, Ref. 11, models I and III; Phillips and Rarita, Ref. 11; Rarita and Schwarzschild, Ref. 11.

Contribution of Pion Production by Primary Cosmic-Ray Nucleons to the Interstellar Electron-Positron Flux

John Doher

Research Department, Grumman Aerospace Corporation, Bethpage, New York 11714

(Received 13 July 1972)

The secondary electron-positron component of high-energy cosmic radiation is calculated. Using the Feynman scaling law for the inclusive pion distribution function, it is shown that the secondary positron-electron component will have the same power law as the primary electron component if the proton and electron injection spectra are the same. Numerical estimates are made using an appropriate fit of the pion single-particle distribution function to accelerator data. The π^0 - γ -ray component is also discussed.

I. INTRODUCTION

In attempting to understand the origin of cosmic-ray electrons, it is necessary to know what percentage of the total flux observed at earth is due to electron production by other particles, such as protons, in interaction with interstellar matter. Presumably, this component of the spectrum may be separated from a so-called primary production

process occurring in the injection period of the cosmic-ray acceleration processes. If we know the primary all-particle spectrum, then by using our knowledge of the fundamental particle production processes, the secondary spectrum may be calculated assuming that a reasonable source-observation-point propagation mode can be used. In this paper, we show that a recent formulation of particle production processes allows a relatively